# Phototransposition Chemistry of 1-Phenylpyrazole. Experimental and Computational Studies

**James W. Pavlik,* Robert E. Connors,* Douglas S. Burns, and Edyth M. Kurzweil**

*Contribution from the Department of Chemistry, Worcester Polytechnic Institute, Worcester, Massachusetts 01609*

*Received April 14, 1993*

**Abstract:** Photophysical and photochemical properties of 1-phenylpyrazole and 3-,4-, and 5-methyl-1-phenylpyrazoles have been investigated. INDO/S calculations agree with experimental measurements which show that the $S_1$ and $T_1$ states of these compounds are $\pi,\pi^*$ in character. Upon $S_0 \rightarrow S_1(\pi,\pi^*)$ excitation, these 1-phenylpyrazoles undergo phototransposition *via* a $P_4$ permutation pathway. This process is consistent with a mechanism involving initial N–N bond cleavage followed by a 1,2-shift and cyclization to form the 1-phenylimidazole product. The 1,2-shift may occur *via* an undetected azirine intermediate. Whereas the regioselectivity of the reaction may be due to the stability of the *N*-phenyl radical, the quantum efficiencies of reaction and fluorescence are remarkably dependent on the location of the methyl group in the pyrazole ring. AM1 calculations provide energy-minimized structures for the more reactive 1-phenylpyrazole and 4-methyl- and 5-methyl-1-phenylpyrazoles in which the phenyl and pyrazole rings are perpendicular as required to stabilize the transition state for N–N bond cleavage. In contrast, such a perpendicular energy minimized $S_1$ structure could not be obtained for the least reactive $S_1(\pi,\pi^*)$ 3-methyl-1-phenylpyrazole which undergoes mainly radiative return to the ground state.

## Introduction

1-Methylpyrazoles are known to undergo phototransposition to 1-methylimidazoles and photocleavage to *N*-methylenaminonitriles.[1-5] Although upon prolonged photolysis, *N*-methylenaminonitriles undergo photocyclization to 1-methylimidazoles,[3,5,6] this reaction is very inefficient and does not account for a significant amount of 1-methylimidazole formation under conditions of short-duration irradiation.[5] Under these latter conditions, permutation pattern analysis[7,8] revealed the operation of up to three distinct mechanisms for the transposition of 1-methylpyrazoles to 1-methylimidazoles.[5] Although experimental and computational studies confirmed the details of the structural changes occurring during the transposition and provided insights into the energetics of the excited- and ground-state reaction coordinates,[9] the spectroscopic properties of these compounds precluded investigation of the photochemical and photophysical details of the phototransposition pathways. Since 1-phenylpyrazoles were known to absorb at more convenient wavelengths and to exhibit measurable luminescence,[10-12] a study of their phototransposition chemistry was undertaken. This photochemical investigation has been supported by spectroscopic and computational studies.

## Results and Discussion

Upon direct irradiation in acetonitrile solution, 1-phenylpyrazole (**1**) was observed to undergo phototransposition to 1-phenylimidazole (**2**) and photocleavage to 3-(*N*-phenylamino)propenenitrile (**3**), identified by direct chromatographic and spectroscopic comparison with authentic samples of these compounds. Quantitative GLC analysis showed that after 13 ± 1% of **1** was consumed, the phototransposition product **2** was formed in 61 ± 4% yield while the photocleavage product **3** was formed in 3.0 ± 0.5% yield.[13] This accounts for approximately 65% of the mass in the reaction. No other products could be detected by GLC. Unlike the case of *N*-methylenaminonitriles, which undergo photocyclization to 1-methylimidazoles,[3,5,6] **3** did not undergo photoconversion to 1-phenylimidazole (**2**).

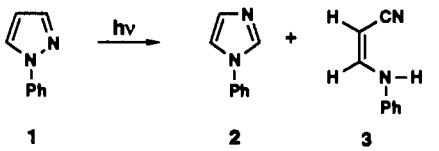


1 2 3 (1)

**Methyl Substitution.** The photochemistry of 1-phenylpyrazoles in which the pyrazole ring carbon atoms were systematically labeled with a methyl group was also investigated. Each isomer, $1.0 \times 10^{-2}$ M in acetonitrile, was irradiated under nitrogen at ambient temperature, and product formation was monitored as a function of irradiation time by using capillary GLC to detect phototransposition products and, after concentration, packed column GLC to detect photocleavage products.

Scheme I shows the primary photoproducts formed upon direct excitation of each methyl substituted 1-phenylpyrazole at 254 nm in acetonitrile solution. In this scheme the numbers in

(1) Tiefenthaler, H.; Dörscheln, W.; Göth, H.; Schmid, H. *Helv. Chim. Acta* **1967**, *50*, 2244–2258.
(2) (a) Beak, P.; Miesel, J. L.; Messer, W. R. *Tetrahedron Lett.* **1967**, 5315–5317. (b) Beak, P.; Messer W. *Tetrahedron* **1969**, *25*, 3287–3295.
(3) Barltrop, J. A.; Day, A. C.; Mack, A. G.; Shahrisa, A.; Wakamatsu, S. *J. Chem. Soc., Chem. Commun.* **1981**, 604–606.
(4) Wakamatsu, S.; Barltrop, J. A.; Day, A. C. *Chem. Lett.* **1982**, 667–670.
(5) Pavlik, J. W.; Kurzweil, E. M. *J. Org. Chem.* **1991**, *56*, 6313–6320.
(6) Ferris, J. P.; Kuder, J. E. *J. Am. Chem. Soc.* **1970**, *92*, 2527–2533.
(7) For a discussion of permutation pattern analysis in aromatic phototransposition chemistry and its application to the analysis of the phototransposition reactions of five-membered heteroaromatics, see: Barltrop, J. A.; Day, A. C. *J. Chem. Soc., Chem. Commun.* **1975**, 177–179. Barltrop, J. A.; Day, A. C.; Moxon, P. D.; Ward, R. W. *J. Chem. Soc., Chem. Commun.* **1975**, 786–787. Barltrop, J. A.; Day, A. C.; Ward, R. W. *J. Chem. Soc., Chem. Commun.* **1978**, 131–133.
(8) For five-membered heterocycles containing two heteroatoms there are 12 different ways of transposing the five ring atoms resulting in 12 permutation patterns identified $P_1$–$P_{12}$. For a table showing these permutation patterns see ref 5.
(9) Connors, R. E.; Pavlik, J. W.; Burns, D. S.; Kurzweil, E. M. *J. Org. Chem.* **1991**, *56*, 6321–6326.
(10) Swaminathan, M.; Dogra, S. K. *Indian J. Chem.* **1983**, *22A*, 853–857.
(11) Swaminathan, M.; Dogra, S. K. *Spectrochim. Acta* **1983**, *39A*, 973–977.
(12) Udachin, Yu. M.; Chursinova, L. V.; Przheval'skii, N. M.; Grandberg, I. I.; Tokmakov, G. P. *Izv. Timiryazevsk. Skh. Akad.* **1980**, 162–169; *Chem. Abstr.* **1980**, *93*, 167052.
(13) All yields in this paper are percent yields determined by quantitative GLC and based on the number of moles of reactant consumed.

0002-7863/93/1515-7645$04.00/0 

Table I. Quantum Yield Results

| reactant | Φ(consumption) | product | Φ(formation) |
|---|---|---|---|
| 1 | 0.19 ± 0.03 | 2 | 0.08 ± 0.01 |
| 4 | <0.01 | 7 | <0.001 |
| 5 | 0.82 ± 0.03 | 8 | 0.20 ± 0.03 |
| 6 | 0.63 ± 0.03 | 9 | 0.34 ± 0.04 |

parentheses represent the absolute quantity of the reactant consumed or the percent yield of the product formed. Thus, unlike 1-methylpyrazoles, which exhibit little regioselectivity in their phototransposition reactions,[5] 1-phenylpyrazoles **4–6** each transpose to a single 1-phenylimidazole product **7–9**, respectively. As in the case of 1-methylpyrazoles,[5] no 1-phenylpyrazole → 1-phenylpyrazole phototranspositions could be detected in these reactions. Finally, the primary 1-phenylimidazole products **7–9** were photostable under these reaction conditions since no subsequent 1-phenylimidazole → 1-phenylimidazole transpositions were detected.

In addtion to phototransposition, both 4-methyl-1-phenylpyrazole (**5**) and 5-methyl-1-phenylpyrazole (**6**) underwent photocleavage to 2-methyl-3-(1-phenylamino)propenenitrile (**10**) and 3-(1-phenylamino)-2-butenenitrile (**11**) in yields of 2% and 9%, respectively. The combined phototransposition and photocleavage product yields account for 60% and 90% of the mass balance in the photolysis of **5** and **6**, respectively.

**Permutation Pattern Analysis.** Considering the positions of the labeled ring atom, methyl-substituted 1-phenylimidazole transposition products **7**, **8**, or **9** were formed by either $P_4$ or $P_7$, $P_4$ or $P_{11}$, or $P_4$ or $P_9$ permutation patterns, respectively. Since it is reasonable to assume that the isomeric methyl-substituted 1-phenylpyrazoles **4–6** isomerize *via* the same transposition mechanism, the simplest inference is that these products are $P_4$ permutation pattern products since this pattern is common to all cases. This permutation pattern was confirmed in the case of 5-methyl-1-phenylpyrazole by monitoring the isomerization of 5-methyl-1-phenylpyrazole-4*d* (**6***d*$_1$). After 70% photoconversion of **6***d*$_1$, $^1$H-NMR analysis of the crude reaction mixture in DMSO-$d_6$ clearly revealed a signal at δ 7.73 for the C-2 ring proton in **9***d*$_1$ with no signal observable for a C-4 proton at δ 6.81. This confirms that the C-3 proton of **6***d*$_1$ has transposed to position 2 in **9***d*$_1$ as required by the $P_4$ permutation pathway.

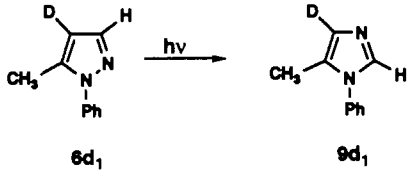


**6d**$_1$ **9d**$_1$ (2)

**Quantum Yields.** The quantum yields for reactant consumption and product formation from the 254-nm photolyses of 1-phenylpyrazole **1** and its monomethyl derivatives **4–6** were determined in triplicate by ferrioxalate actinometry,[14] and are tabulated in Table I. Irradiations were carried out to less than 10% conversion and reactant consumption and product formation were determined by GLC with use of internal standards. As shown in Table I, methyl substitution at C-3 of the pyrazole ring drastically reduces the quantum yield of the reaction while substitution at C-4 or C-5 substantially increases the quantum yield for the phototransposition.

**Sensitized Irradiations.** Sensitized irradiations of 1-phenylpyrazole **1** ($E_T$ = 75.0 kcal/mol based on the 0,0 band of phosphorescence) and methyl substituted 1-phenylpyrazoles **4–6** ($E_T$ = 74.4–77.5 kcal/mol) were carried out in acetone ($E_T$ = 79–82 kcal/mol).[15] All of these 1-phenylpyrazoles were found to be unreactive as triplets.

Scheme I

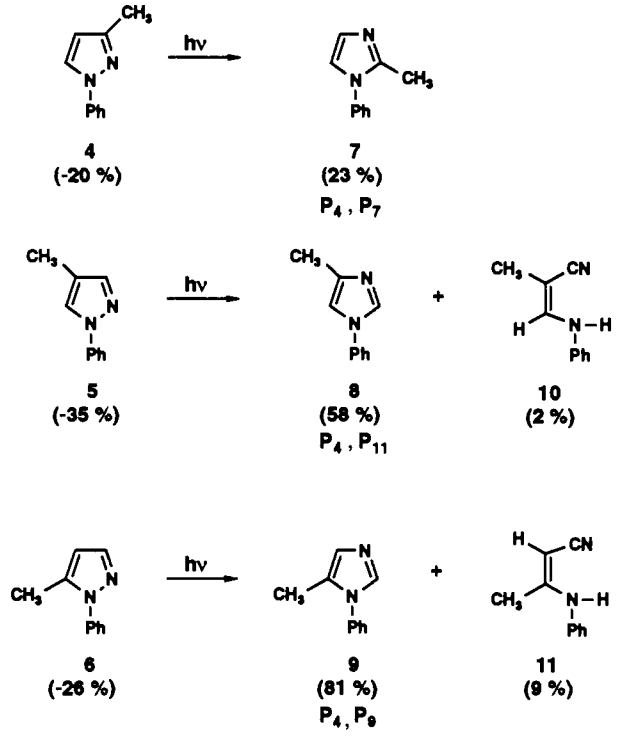


Table II. Experimental and Calculated Wavelengths and Oscillator Strengths for $S_1$

| | $\lambda_{expt}$ | $f_{expt}$ | $\lambda_{calc}$ | $f_{calc}$ |
|---|---|---|---|---|
| 1 | 255 | 0.28 | 252 | 0.25 |
| 4 | 261 | 0.24 | 261 | 0.23 |
| 5 | 262 | 0.25 | 265 | 0.24 |
| 6 | 242 | 0.20 | 253 | 0.15 |

**Spectroscopic Properties.** In order to better understand the excited states of these 1-phenylpyrazole compounds, a series of spectroscopic and computational investigations have been carried out. Room temperature absorption spectral data for compounds **1**, **4**, **5**, and **6** in acetonitrile are summarized in Table II. Spectra for the four molecules are broad and without well-defined vibrational structure. INDO/S semiempirical molecular orbital calculations with 91 singly and 106 doubly excited configurations were carried out. As seen from Table II, excellent agreement between the experimental and calculated energies and oscillator strengths for $S_1$ has been obtained. For the four 1-phenylpyrazoles, $S_1$ arises primarily from a HOMO → LUMO excitation with electron density delocalized throughout the entire molecule for both MO's, whereas $S_2$ arises primarily from HOMO → LUMO+1 with electron density restricted to the phenyl ring for the upper MO. The blue shift of $S_1$ for **6** compared to **1**, **4**, and **5** is consistent with AM1 optimized geometries for $S_0$. These calculations predict that in the fully optimized $S_0$ geometries of 1-phenylpyrazoles the pyrazole and phenyl rings are twisted about the N–C bond joining them. The dihedral angle between the planes of the two rings is calculated to be 26° for **1**, **4**, and **5**, but increases to 40° for **6**, presumably because of the increased steric interaction brought about by methyl substitution at the 5 position of the pyrazole ring. This greater angle of twist between the rings results in decreased conjugation and a higher excitation energy for **6**.

(14) Hatchard, C. G.; Parker, C. A. *Proc. R. Soc. London, Ser. A* **1956**, *23*, 518–536.

(15) Schmidt, M. W.; Lee, E. K. C. *J. Am. Chem. Soc.* **1970**, *92*, 3579–3586.

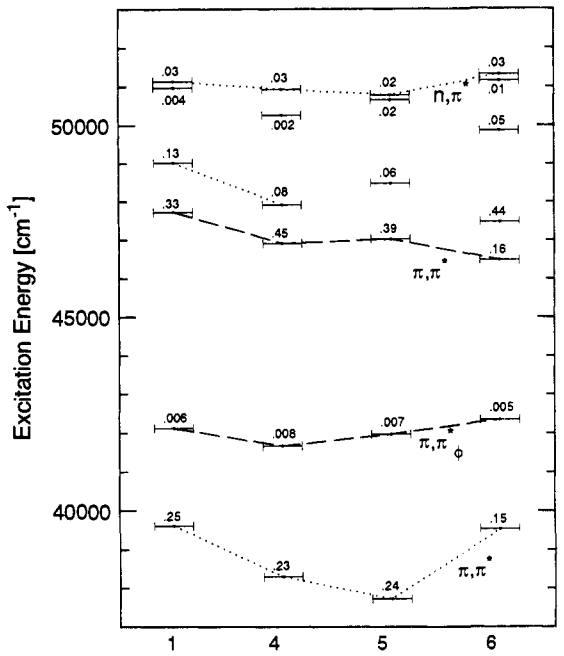


**Figure 1.** Correlation diagram of excited singlet states computed by INDO/S for **1**, **4**, **5**, and **6**. Oscillator strengths are given for each state.

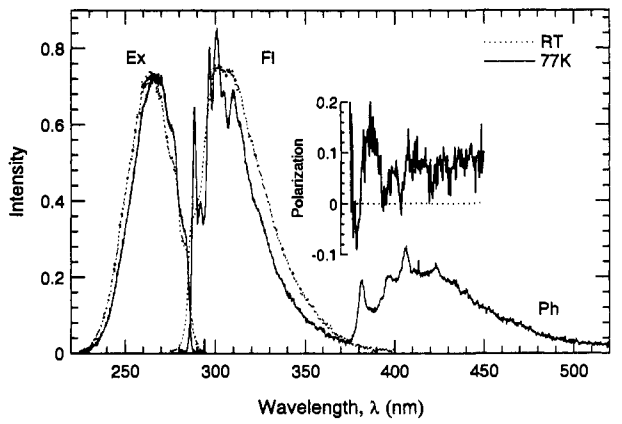


**Figure 2.** Fluorescence excitation, fluorescence, phosphorescence, and polarized phosphorescence spectra of **1** in MCH at room temperature and 77 K.

The first n → π* transition for **1** and **4**–**6** is predicted to occur in the 195–200 nm region. A diagram correlating the excited singlet states calculated to occur at wavelengths longer than 195 nm is presented in Figure 1. The numbers with each state indicate the predicted oscillator strength for the transition. These data show that the n → π* transition is at significantly higher energy than the π → π* $S_1$ and $S_2$ transitions. Furthermore, these $S_1$ and $S_2$ transitions are either delocalized throughout the entire molecule ($S_1$) or entirely localized in the phenyl ring ($S_2$).

Excitation and emission spectra of **1** were measured in methylcyclohexane (MCH) at room temperature and at 77 K and are presented in Figure 2. The room temperature excitation and fluorescence spectra show a mirror image relationship with small Stokes shift. The fluorescence spectrum at 77 K shows significantly more vibrational structure with a prominent 0,0 band at 288.5 nm (98.8 kcal/mol), whereas the 77 K excitation spectrum does not change significantly from the broad spectrum observed at room temperature. The 0,0 band of phosphorescence indicates a high energy triplet state which is located at 379.9 nm (75.0 kcal/mol). Compounds **1**, **4**, and **5** have spectra which are similar in structure and energy. Furthermore, they have nearly the same ratio of fluorescence to phosphorescence (≈2:1). The spectrum of compound **6** has the same general shape as that of compounds **1**, **4**, and **5**, however vibrational structure is less resolved, and the ratio of fluorescence to phosphorescence is greatly reduced (≈0.25:1). Photophysical data of compounds **1** and **4**–**6** in acetonitrile are summarized in Table III. Intrinsic fluorescence lifetimes ($\tau_f^{\circ}{}_{SB}$) have been determined from Strickler–Berg calculations in which the areas under the absorption and emission curves are determined.[16] Results of these calculations are in reasonable agreement with intrinsic lifetimes calculated from $\tau_f^{\circ} = \tau_f/\Phi_f$ for compounds **1**, **4**, and **5**, suggesting that the absorbing and emitting states are the same and that the INDO/S calculations have predicted $S_1$ correctly. In the case of compound **6**, there is a significant difference between $\tau_f^{\circ}$ and $\tau_f^{\circ}{}_{SB}$ (18 vs 3.8 ns). This disagreement could be due to a breakdown of the Strickler–Berg model for systems which undergo a large geometric change upon excitation.[16] AM1 calculations of **6** show a significant change in twist angle between rings, going from 40° in $S_0$ to either 20° or 90° in $S_1$.

**Table III.** Photophysical Data for 1-Phenylpyrazoles in Acetonitrile

| | $\Phi_f$ | $\tau_f$ (ns) | $\tau_f^{\circ}$ (ns) | $\tau_f^{\circ}{}_{SB}$ (ns) | $\tau_p$[a] (s) | $k_f \times 10^{-7}$ ($s^{-1}$) | $\Phi_{pyr}$ | $\Phi_{imi}$ | $k_r \times 10^{-7}$ ($s^{-1}$) |
|---|---|---|---|---|---|---|---|---|---|
| **1** | 0.56 | 1.94 | 3.5 | 2.9 | 4.2 | 29 | 0.19 | 0.075 | 3.9 |
| **4** | 0.75 | 1.93 | 2.6 | 3.2 | 4.0 | 39 | <0.01 | <0.001 | 0.052 |
| **5** | 0.24 | 0.29 | 1.2 | 3.2 | 4.2 | 83 | 0.82 | 0.20 | 69 |
| 6 | 0.097 | 1.72 | 18 | 3.8 | 2.0 | 5.6 | 0.63 | 0.34 | 20 |

[a] MCH solvent.

The values of the radiative rate constants for fluorescence and the rate constants for formation of imidazole, presented in Table III, have been calculated from $k_f = \Phi_f/\tau_f$ and $k_r = \Phi_{imi}/\tau_f$. Compound **4**, which is highly fluorescent ($\Phi_f = 0.75$) and nonreactive ($\Phi_{pyr} < 0.01$), has the smallest $k_r$. Compound **6**, which is fairly reactive ($\Phi_{pyr} = 0.63$) and not very fluorescent ($\Phi_f = 0.097$), is the only compound in which $k_r$ is larger than $k_f$.

Although triplet states are not directly implicated in the photochemical reactions discussed here, their spectroscopic properties have been investigated to provide a more complete description of 1-phenylpyrazole excited states. Phosphorescence lifetimes $\tau_p$ presented in Table III were obtained in MCH at 77 K by evaluating the decay of the exponential for at least 2–3 lifetimes. Compounds **1**, **4**, and **5** have lifetimes on the order of 4 s; whereas compound **6**, the only pyrazole in which $\Phi_p > \Phi_f$ at 77 K, has a lifetime of 2 s. The long lifetimes of these molecules indicate phosphorescence from a π,π* triplet state. INDO/S calculations of the AM1 optimized $S_0$ geometry predict that $T_1$ is π,π* arising primarily from a mixture of HOMO → LUMO and (HOMO−1) → LUMO configurations. The greater $\Phi_p/\Phi_f$ ratio and shorter lifetime for **6** compared to **1**, **4**, and **5** is consistent with more efficient spin–orbit coupling between $T_1$ and $S_1$. This can be seen to arise as a result of the large angle of twisting between the two rings in **6** producing a mixing of σ and π orbitals such that non-zero one-center spin–orbit coupling matrix elements survive for the direct spin–orbit coupling of $^1(\pi,\pi^*)$ to $^3(\pi,\pi^*)$ states.

Phosphorescence and polarized phosphorescence spectra have been measured for **1** and are presented in Figure 2. The 0,0 band and several presumably totally symmetric vibronic bands have negative polarization when exciting $S_1$, whereas the remainder of the spectrum has positive polarization. Similar results in which in-plane polarization is observed outside of the 0,0 band have been obtained for other heteroaromatic molecules and are indicative of a second-order vibronic spin–orbit coupling mechanism in which the $S_1$ and $T_1$ π,π* states are mixed through an intermediate n,π* state.[17] INDO/S calculations of the location of $^{1,3}(n,\pi^*)$ states suggest that the second-order mechanism involving vibronic coupling in the triplet manifold is of greater importance than the mechanism involving vibronic coupling in

(16) Strickler, S. J.; Berg, R. A. *J. Chem. Phys.* **1962**, *37*, 814–822.
(17) Lim, E. C. In *Excited States*; Lim, E. C., Ed.; Academic Press: New York, 1977; Vol. 3.

**Scheme II**

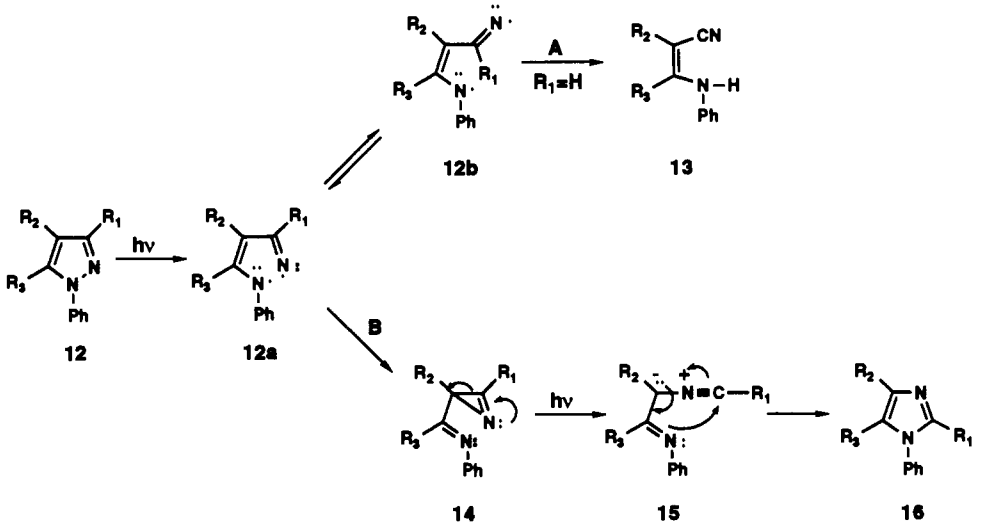


**Scheme III**

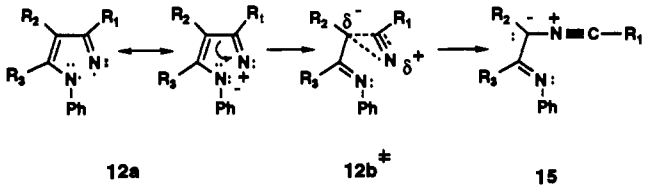


the singlet manifold. The out-of-plane polarization observed at the 0,0 band and totally symmetric vibrations is likely due to first-order spin–orbit coupling of $T_1$ with the lowest energy $^1(n,\pi^*)$ state.[18] Calculations indicate that $^1(n,\pi^*)$ is the first excited singlet state with out-of-plane polarization. The mixing of $n,\pi^*$ character into $T_1$ is supported by solvent effects on $\tau_p$. Upon changing the solvent from MCH to ethanol, $\tau_p$ increases from 4.2 to 4.9 s. This change in lifetime is consistent with less efficient first- and second-order spin–orbit coupling involving $n,\pi^*$ and $T_1(\pi,\pi^*)$ states due to a solvent induced blue shift of the $n,\pi^*$ states thus producing an increase in the energy gap between $n,\pi^*$ states and $T_1$.[18]

**Mechanistic Discussion.** The $P_4$ pyrazole → imidazole phototransposition and the pyrazole → enaminonitrile photocleavage have been rationalized by initial photochemical cleavage of the N–N bond in the pyrazole ring resulting in biradical species **12a**.[1-5] The two pathways shown in Scheme II can be envisioned for this species. First, in the presence of a hydrogen at C-3 of the pyrazole ring ($R_1$ = H), rotation about the C-3–C-4 bond to conformation **12b** followed by H-atom transfer (Path A) from C-3 to N-1 would yield the observed enaminonitrile **13**. Considering the low yields of enaminonitriles formed upon irradiation of 1-phenylpyrazoles, this must constitute a minor reaction pathway.

As originally suggested by Schmid and co-workers,[1] such a diradical species could cyclize (Path B) to *N*-phenylimino-*2H*-azirine **14**. Although such azirines have never been detected as intermediates in the pyrazole → imidazole phototransposition, several facts support their existence. First, acylazirines **18** are well-established intermediates in the analogous $P_4$ phototrans-

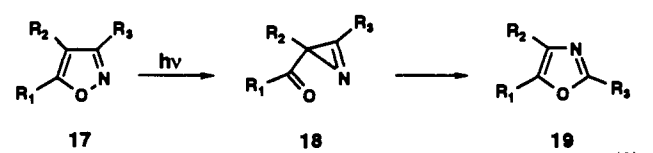


(3)

(18) Lim, E. C.; Yu, J. M. H. *J. Chem. Phys.* **1967**, *47*, 3270–3275.

position of isoxazole **17** to oxazole **19**.[19] Second, one such iminoazirine, 3-phenyl-2-(*N*-phenylimino)-*2H*-azirine (**20**), has been independently synthesized and shown to undergo efficient photoisomerization to 1,2-diphenylimidazole (**22**)[20] *via* nitrile ylide **21**.[21] Thus, if 1-phenylpyrazole **12** (Scheme II) undergoes

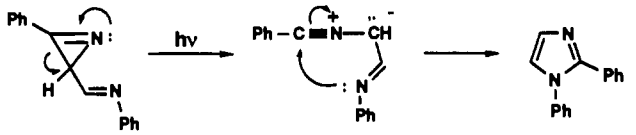


(4)

photo-ring contraction to (*N*-phenylimino)azirine **14**, this species would be expected to undergo efficient photo-ring expansion to 1-phenylimidazole **16** *via* nitrile ylide **15**.

As shown in Scheme III, however, the net effect of azirine formation and ring-opening to the nitrile ylide is a 1,2-shift of C-3 from C-4 to N-2. Such a 1,2-shift could be envisioned directly[22] *via* a transition state **12b‡** having considerable azirine character. Accordingly, an azirine-type entity may be a reactive species on the transposition reaction coordinate rather than an isolable intermediate.

The enhanced regioselectivity of the 1-phenylpyrazole phototransposition as compared to the 1-methylpyrazole phototransposition may be due to the greater stability of the *N*-phenyl radical produced by photolytic N–N bond cleavage in 1-phenylpyrazoles as compared to the *N*-methyl radical produced from 1-methylpyrazole. Presumably, this greater stability due to odd electron delocalization into the phenyl ring in **12a** would also lower the energy barrier for N–N cleavage by lowering the energy of the incipient radical in the transition state. For this to occur, overlap

(19) (a) Kurtz, D. W.; Schechter, H. *J. Chem. Soc., Chem. Commun.* **1966**, 689–690. (b) Ullman, E. F.; Singh, B. *J. Am. Chem. Soc.* **1966**, *88*, 1844–1845; **1967**, *89*, 6911–6916. (c) Singh, A.; Zweig, A.; Gallivan, J. B. *J. Am. Chem. Soc.* **1972**, *94*, 1199–1206. (d) Nishiwaki, T.; Nakano, A.; Matsuoka, H. *J. Chem. Soc. C* **1970**, 1825–1829. (e) Nishiwaki, T.; Fujiyama, F. *J. Chem. Soc., Perkin Trans. 1* **1972**, 1456–1459. (f) Wamhoff, H. *Chem. Ber.* **1972**, *105*, 748–752. (g) Sato, T.; Yamamoto, K.; Fukui, K. *Chem. Lett.* **1973**, 111–114. (h) Goeth, H.; Gagneux, A. R.; Eugster, C. H.; Schmid, H. *Helv. Chim. Acta* **1967**, *50*, 137–142. (i) Padwa, A.; Chen, E.; Kua, A. *J. Am. Chem. Soc.* **1975**, *97*, 6484–6491. (j) Dietliker, K.; Gilgen, P.; Heimgartner, H.; Schmid, H. *Helv. Chim. Acta* **1976**, *59*, 2074–2099.

(20) Padwa, A.; Smolanoff, J.; Tremper, A. *Tetrahedron Lett.* **1974**, 29–32; *J. Am. Chem. Soc.* **1975**, *97*, 4682–4691.

(21) (a) Padwa, A. *Acc. Chem. Res.* **1976**, *9*, 371–378. (b) Griffin, G. W.; Padwa, A. In *Photochemistry of Heterocyclic Compounds*; Buchardt, O., Ed.; John Wiley and Sons: New York, 1976.

(22) Padwa, A.; Chen, E.; Kua, A. *J. Am. Chem. Soc.* **1975**, *97*, 6484–6491.

**Table IV.** Heat of Formation (kcal/mol) and Twist Angle (deg) (in Parentheses) for 1-Phenylpyrazoles in $S_0$ and $S_1$ Calculated by AM1

| | 1 | 4 | 5 | 6 |
|---|---|---|---|---|
| $S_0$ | 105 (26[b]) | 97 (26) | 96 (26) | 98 (40) |
| $S_1$ (FC)[a] | 213 (26) | 204 (26) | 203 (26) | 208 (40) |
| $S_1$[b] | 207 (6) | 200[e] | 199 (8) | 202 (20) |
| $S_1$[c] | 202 | 194 | 193 | 195 |
| $S_1$[d] | 192 (87)[f] | | 195 (87) | 196 (87) |

[a] FC, Franck–Condon vertical energy (ground-state geometry). [b] Planar phenyl ring. [c] Distorted phenyl ring (benzvalene-like geometry). [d] Rings twisted 90°. [e] Phenyl ring slightly distorted. [f] N–N bond order = 0.2.

of the $\sigma$-orbitals of the N–N bond with the p-orbitals of the benzene ring would require a transition state geometry (**12‡**) in which the two rings are perpendicular.

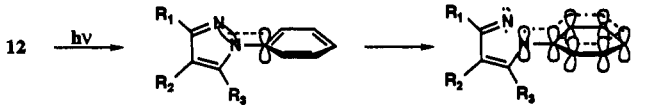


(5)

While the *N*-phenyl group greatly influences the regioselectivity of the reaction, methyl substitution in the pyrazole ring greatly influences the efficiency of the photoreaction (Table I). AM1 calculations have provided insights into why this is the case. The predicted heats of formation and angle of twist between the phenyl and pyrazole rings for **1** and **4–6** on both $S_0$ and $S_1$ are summarized in Table IV.

Geometry optimization on $S_1$ revealed more than one energy minimum for **1** and **4–6**. The computed ground-state geometries were used as the starting points for Franck–Condon calculations and the resulting molecules were then allowed to optimize to an $S_1$ geometry. For 1-phenylpyrazoles **5** and **6**, geometries **5a** and **6a** were obtained in which the angle of twist between the pyrazole and phenyl rings decreased from 26° in **5** to 8° in **5a** or from 40° in **6** to 20° in **6a**. This more planar conformation would not be consistent with the geometrical requirement for electron delocalization in the phenyl ring. In addition to these more coplanar structures, $S_1$ geometries in which the two rings are twisted by 87°, **1c**, **5c**, and **6c**, could be optimized for **1**, **5**, and **6** by starting with structures in which the two rings are perpendicular. As shown in Table IV, these almost perpendicular $S_1$ structures **1c**, **5c**, and **6c** are calculated to be 15, 4, and 6 kcal/mol more stable than the less twisted $S_1$ structures **1a**, **5a**, and **6a**. This suggests that the two $S_1$ energy minimized structures **1a** and **1c**, **5a** and **5c**, and **6a** and **6c** are separated by energy barriers which are surmountable in the solution phase.

Interestingly, AM1 calculations reveal that excitation of **1** to the energy minimized perpendicular $S_1$ state **1c** is accompanied by an increase in the N–N bond length from 1.35 Å in $S_0$ to 1.78 Å in **1c**. This increase in bond length corresponds to a change in the N–N bond order from 1.12 in **1** to 0.38 in **1c** and indicates that the N–N bond is essentially broken in **1c**. It is of further interest to note that excitation is also accompanied by a change in the electronic charge in the phenyl ring from +0.12 in **1** to –0.08 in **1c**, consistent with electron delocalization into the phenyl ring. Finally, although our earlier MNDO calculations reveal that the pyrazole ring in 1-methylpyrazole undergoes disrotatory deformation upon $S_0 \rightarrow S_1$ excitation,[9] these AM1 calculations predict that in 1-phenylpyrazole (**1**) the pyrazole ring remains planar upon excitation. This is consistent with the observed lack of reactivity *via* the electrocyclic ring closure–nitrogen walk pathway in the latter compound.

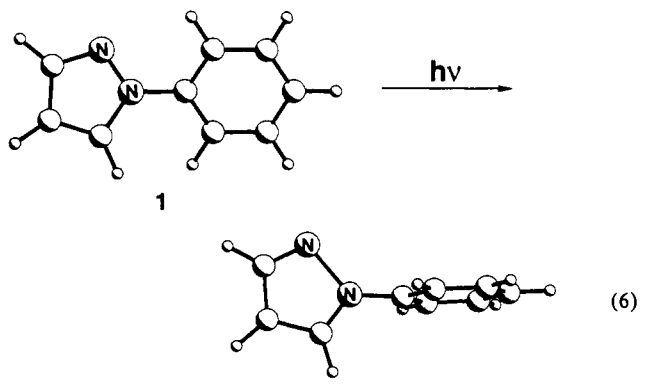


(6)

AM1 calculations reveal similar changes upon excitation of **5** and **6** to their perpendicular $S_1$ states **5c** and **6c**. Thus, N–N bond lengths are calculated to increase from 1.35 Å in **5** and **6** to 1.47 Å in **5c** and **6c** corresponding to changes in the N–N bond orders from 1.12 in **5** and **6** to 0.85 and 0.86 in **5c** and **6c**, respectively. Thus again, these calculations predict that the N–N bonds are weakened in the perpendicular $S_1$ states **5c** and **6c**. Furthermore, in the perpendicular conformations **5c** and **6c**, simulation of bond cleavage by increasing the N–N bond length results in a decrease in the energies of the structures. This is consistent with stabilization of the incipient radical *via* electron delocalization into the phenyl ring. Indeed, calculations show that the total charge on the phenyl ring for **5c** becomes more negative as it changes from +0.06 to –0.11 when the N–N bond length is increased from 1.47 to 1.55 Å.

It is also instructive to note that such a perpendicular $S_1$ conformation could not be optimized for the least photoreactive 3-methyl-1-phenylpyrazole (**4**). In the cases of **1** and **4**, optimization of the Franck–Condon $S_1$ geometries led to structures **1b** and **4b** in which the phenyl rings are severely distorted. Although when the starting geometry of **1** is not twisted it is

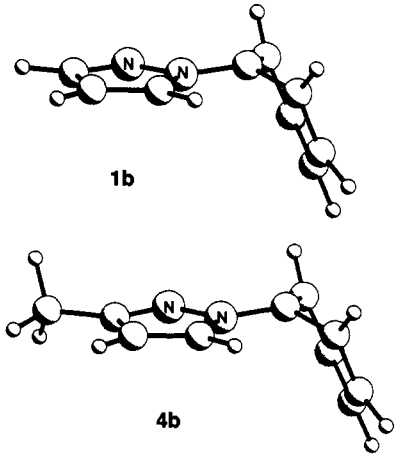


possible to obtain an energy minimized less-twisted structure containing a planar phenyl ring **1a**, it has not been possible to locate an optimized structure for **4** in which the phenyl ring is completely planar **4a**. In this case, the phenyl ring is still bent, but less so than when starting with the Franck–Condon structure for **4**. $S_1$ optimization for **4** was also carried out by beginning with a planar phenyl ring twisted 90° from the pyrazole ring. Although optimizations of such structures for **1**, **5**, and **6** led to energy minimized perpendicular structures **1c**, **5c**, and **6c**, in the case of **4**, optimization led to the same benzvalene-like structure that was found when starting with the ground-state geometry of **4**.

Failure to attain the perpendicular conformation for **4** in $S_1$ thus precludes efficient overlap of the N–N $\sigma$-orbital of the pyrazole ring with the p-orbitals of the phenyl moiety. This would be expected to significantly increase the energy barrier for the

N–N bond cleavage and is consistent with the drastically decreased reaction efficiency observed for **4** as compared to **1**, **5**, and **6**. In the absence of photocleavage of the N–N bond, the major pathway for deactivation of the $S_1$ state of **4** is luminescence as evidenced by the high quantum efficiency for fluorescence, $\Phi_f = 0.75$ for **4** as compared to values of 0.56, 0.24 and 0.097 respectively for **1**, **5**, and **6**.

In view of the energy minimized $S_1$ structures for **4** bearing a distorted phenyl ring, it is tempting to suggest that its lower photoreactivity is due to the excitation energy being localized in the phenyl ring and that phenyl ring distortion contributes to the deactivation of these 1-phenylpyrazoles, perhaps *via* a benzvalene intermediate. Several theoretical and experimental observations are not consistent with this conclusion. Thus, whereas INDO/S calculations predict such energy localization in $S_2$ (Figure 1), the same calculations indicate that the $S_1$ molecular orbital is delocalized throughout the entire molecule. Furthermore, the large quantum yields for fluorescence and the small Stokes shifts are consistent with small geometrical differences between the absorbing and emitting species. It is possible, however, that phenyl ring deformation constitutes a minor pathway for radiationless decay in these molecules. Indeed, AM1 calculations indicate that the energy gap between $S_1$ and $S_0$ potential energy surfaces for the benzvalene-like structure of **1** ($\Delta E_{S_1-S_0}$ = 38 kcal/mol) is much smaller than when the phenyl ring remains planar ($\Delta E_{S_1-S_0}$ = 98 kcal/mol).

## Conclusions

Photophysical properties of 1-phenylpyrazole and methyl substituted 1-phenylpyrazoles have been investigated using experimental and computational methods. INDO/S calculations agree well with experimental measurements and show that $S_1$ and $T_1$ are of $\pi,\pi^*$ character. Fluorescence quantum yields and lifetimes exhibit a considerable dependence on the position of methyl substitution. Polarized phosphorescence spectra, phosphorescence lifetime measurements, and INDO/S calculations indicate that $T_1$ and $S_1$ are mixed through vibronic spin–orbit coupling involving an intermediate $n,\pi^*$ state. These results help us to better understand and support the photochemical findings.

1-Phenylpyrazole (**1**) and methyl-substituted 1-phenylpyrazoles **4–6** undergo phototransposition to 1-phenylimidazole (**2**) or methyl-substituted 1-phenylimidazoles **7–9** *via* a $P_4$ permutation pathway. This permutation process is consistent with a mechanism involving initial N–N bond cleavage followed by a 1,2-shift of C-4 from C-3 to N-2 and cyclization of the nitrile ylide to form the 1-phenylimidazole product. The 1,2-shift may occur *via* an undetected azirine intermediate. Whereas the regioselectivity of the reaction may be due to stability of the *N*-phenyl radical produced upon photocleavage of the N–N bond, the quantum efficiency of the reaction is remarkably dependent on the location of the methyl substituent in the pyrazole ring. Thus, whereas methyl substitution at position 4 or 5 is accompanied by an increase in the quantum yield, methyl substitution at position 3 greatly reduces the transposition efficiency. These substituent effects can be rationalized by the $S_1$ geometries determined from AM1 calculations. Thus, $S_1$ structures for the more reactive 1-phenylpyrazole (**1**) and 4-methyl- and 5-methyl-1-phenylpyrazoles (**5** and **6**) could be optimized in which the phenyl and pyrazole rings are perpendicular as required to stabilize the transition state for N–N bond cleavage. In contrast, such a perpendicular energy minimized $S_1$ structure could not be obtained for the least reactive **4**. This precludes effective overlap of the N–N $\sigma$-orbital of the pyrazole ring with the p-orbitals of the phenyl moiety which would be expected to substantially increase the energy barrier for N–N cleavage and phototransposition.

## Experimental Section

**General Procedures.** $^1H$ and $^{13}C$ NMR spectra were recorded at 200 and 52.3 MHz on a Bruker FT-NMR system. $^1H$ and $^{13}C$ chemical shifts were measured relative to internal $Me_4Si$ and $CHCl_3$, respectively. Infrared spectra were recorded on a PE-1720 FT spectrometer. GLC was performed on a PE-8500 FID instrument equipped with a 30 m × 0.25 mm i.d. fused silica column coated with 0.25 $\mu$ Supelcowax 10 bonded phase (Column A) or on a PE-3920 FID instrument using a 6 ft × $^1/_8$ in. column packed with 2% OV-225 on Chromosorb G (Column B) or a 6 ft × $^1/_4$ in. column packed with 2% Carbowax 20M-TPA on Chromosorb G (Column C) for preparative scale work. Mass spectra were recorded with an HP 5970B mass selective detector interfaced to an HP 5880 capillary gas chromatograph. Elemental analyses were determined by Desert Analytics, Tucson, AZ.

**Spectroscopic Measurements.** The apparatus for measuring luminescence and polarized luminescence spectra has been described previously.[23] Phosphorescence lifetimes were measured by monitoring the decay of the phosphorescence intensity with time. Fluorescence data for quantum yield measurements were obtained on a Perkin-Elmer LS50 Luminescence spectrometer. Fluorescence quantum yields were measured relative to *p*-xylene in methylcyclohexane ($\Phi_f$ = 0.33, $\lambda_{ex}$ = 260 nm).[24] Samples were degassed by bubbling dry nitrogen for a minimum of 10 min.

**Method of Calculation.** All AM1[25] calculations were performed with a DECstation 5000/200 computer operating the MOPAC[26] program with standard parameters. In general, structures obtained from PCMODEL[27] were the starting points for AM1 optimizations using standard minimization techniques and internal coordinates. Calculations of excitation energies and oscillator strengths were carried out by using the INDO/S[28] semiempirical MO method with configuration interaction.

**Starting Materials and Products.** 1-Phenylpyrazole (**1**), 3-methyl-1-phenylpyrazole (**4**), and 1-phenylimidazole (**2**), 3-ethoxyacrylonitrile, and 3-aminocrotononitrile were available from Aldrich Chemical Co. 3-(*N*-Phenylamino)-2-butenenitrile (**11**) was prepared from 3-aminocrotonitrile and aniline.[29]

**4-Methyl-1-phenylpyrazole (5).** Phenylhydrazine (1.8 g, 0.017 mol) in 35 mL of 90% ethanol was cooled to 0 °C and 1 mL of concentrated $H_2SO_4$ was added dropwise. After the resulting solution was warmed to room temperature, 1,1,3,3-tetraethoxy-2-methylpropane[30] (7.8 g, 0.034 mol) was added dropwise and the mixture was refluxed for 3 h, allowed to cool to room temperature, and neutralized to pH 7 with $Na_2CO_3$. The resulting solution was extracted with $CH_2Cl_2$ (3 × 20 mL), dried ($Na_2SO_4$), and concentrated, and the residue was distilled to give 4-methyl-1-phenylpyrazole as a colorless oil: bp 98–99 °C (1.8 Torr) (lit.[31] bp 98–100 °C at 1.5 Torr); 2.1 g (0.013 mol, 80% yield); $^1H$ NMR (DMSO-$d_6$) $\delta$ 2.09 (s, 3H), 7.1–7.7 (m, 7H); $^{13}C$ NMR ($CDCl_3$) $\delta$ 8.6, 117.9, 118.3, 125.0, 125.7, 129.1, 140.0, 141.5; IR (neat) 3150, 3116, 3096, 2973, 2921, 1955, 1872, 1699, 1600, 1574, 1505, 1462, 1424, 1403, 1386, 1358, 1251, 1219, 1183, 1153, 1072, 1025, 952, 902, 855, 799 cm$^{-1}$; UV($CH_3CN$) 263 nm ($\epsilon$ 14 500).

**5-Methyl-1-phenylpyrazole (6).** To a solution of 1-phenylpyrazole (0.86 g, 6.0 mmol) in 30 mL of dry THF at −78 °C under argon was slowly added a solution of *n*-butyllithium (2.0 M in *n*-pentane, 4.5 mL, 9.0 mmol). After the solution was stirred for 1 h at −78 °C, methyl iodide (5.0 mL, 0.060 mol) was added and the resulting mixture was allowed to warm to room temperature. This solution was concentrated, 20 mL of water was added, and this solution was then extracted with ether (3 × 10 mL). The combined extracts were dried ($Na_2SO_4$), concentrated, and distilled (Kugelröhr) to provide 5-methyl-1-phenylpyrazole as a colorless oil: bp (oven temperature) 155 °C (12 Torr) (lit.[32] 87–88 °C at 0.9 Torr); 0.69 g (4.4 mmol, 73% yield); $^1H$ NMR ($CDCl_3$) $\delta$ 2.31 (s, 3H), 6.20 (s, 1H), 7.3–7.5 (m, 5H), 7.59 (s, 1H); $^{13}C$ NMR ($CDCl_3$) $\delta$ 12.1, 106.7, 124.5, 127.3, 128.8, 138.3, 139.6; IR (neat) 3100, 3067,

(23) Connors, R. E.; Sweeney, R. J.; Cerio, F. *J. Phys. Chem.* **1987**, *92*, 819–822.
(24) Shold, D. M. *Chem. Phys. Lett.* **1977**, *49*, 243–246.
(25) Dewar, M. J. S.; Zoebisch, E. G.; Healy, E. F.; Stewart, J. J. P. *J. Am. Chem. Soc.* **1985**, *107*, 3902–3909.
(26) Available from the Quantum Chemistry Program Exchange: MOPAC, version 5, QCPE 455.
(27) PCMODEL, force field calculation based on the MM2 method (N. L. Allinger), Serena Software, Box 3076, Bloomington, IN 47402-3076.
(28) Ridley, J.; Zerner, M. *Theor. Chim. Acta* **1973**, *32*, 111–134.
(29) Dedina, J.; Kuthen, J.; Palcek, J.; Schrami, J. *Collect. Czech. Chem. Commun.* **1975**, *40*, 3476–3490.
(30) Klimko, V. T.; Skoldinov, A. P. *Zh. Obshch. Khim.* **1959**, *29*, 4027–4029; *Chem. Abstr.* **1960**, *54*, 20870a.
(31) Klimko, V. T.; Protopopova, T. V.; Skoldinov, A. P. *Zh. Obshch. Khim.* **1961**, *31*, 170–175; *Chem. Abstr.* **1961**, *55*, 22291f.
(32) Micetich, R. G.; Baker, V.; Spevak, P.; Hall, T. W.; Bains, B. K. *Heterocycles* **1985**, *23*, 943–951.

2983, 2961, 2931, 1743, 1600, 1545, 1502, 1455, 1391, 1267, 1206, 1121, 1073, 1036, 1016, 923, 766 $cm^{-1}$; UV($CH_3CN$) 242 nm ($\epsilon$ 11 300); MS *m/e* (%) 158 (100), 157 (70), 130 (52), 90 (14), 78 (14), 77 (77), 64 (12), 63 (13), 52 (14), 51 (72), 50 (23).

**5-Methyl-4-deuterio-1-phenylpyrazole (6$d_1$).** 5-Methyl-1-phenylpyrazole (1.0 g, 6.3 mmol) in $D_2SO_4$ (4.0 mL, 70% in $D_2O$) was maintained at 70 °C while being protected from atmospheric moisture. After 4 days $^1H$ NMR indicated 95% deuteration at C-4. The resulting solution was added dropwise to a stirred suspension of sodium bicarbonate (10 g) in water (10 mL). Enough water was added to dissolve the resulting solid and the solution was extracted with $CH_2Cl_2$ (3 × 10 mL). The combined extracts were dried ($Na_2SO_4$) and concentrated, and the residue was purified by distillation (Kugelröhr) to give 5-methyl-4-deuterio-1-phenylpyrazole as a colorless oil: bp (oven temperature) 150 °C (15 Torr); 0.78 g (4.9 mmol, 78% yield); $^1H$ NMR ($CDCl_3$) $\delta$ 2.33 (s, 3H), 7.3–7.5 (m, 5H), 7.59 (s, H-3); MS *m/e* (%) 159 (100), 158 (75), 157 (9.0), 131 (45), 130 (15), 118 (11), 91 (15), 90 (13), 78 (17), 77 (91), 65 (11), 64 (15), 63 (16), 51 (87), 50 (29), 40 (25), 39 (37).

**2-Methyl-1-phenylimidazole (9).** To a stirred solution of 1-phenylimidazole (0.86 g, 6.0 mmol) in 30 mL of dry THF at −78 °C was slowly added *n*-butyllithium (2.0 M in *n*-pentane, 6.0 mL, 12 mmol). After the solution was stirred for 1 h at −78 °C, methyl iodide (5.0 mL, 0.060 mol) was added. The solution was then stirred for 15 min and allowed to warm to room temperature. The resulting solution was concentrated, 25 mL of water was added, and this solution was then extracted with ether. The combined extracts were dried ($Na_2SO_4$) and concentrated, and the residual oil was distilled (Kugelröhr) to provide 2-methyl-1-phenylimidazole as a colorless oil: bp (oven temperature) 165 °C (12 Torr) (lit.[33] bp 142 °C at 15 Torr); 0.55 g (3.5 mmol, 58% yield); $^1H$ NMR (DMSO-$d_6$) $\delta$ 2.37 (s, 3H), 6.91 (s, 1H), 7.22 (s, 1H), 7.2–7.5 (m, 5H); $^{13}C$ NMR ($CDCl_3$) $\delta$ 13.5, 120.4, 125.2, 127.4, 127.9, 129.2, 137.7, 143.3; IR (neat) 3387, 3063, 2961, 1677, 1640, 1599, 1525, 1503, 1455, 1417, 1376, 1303, 1179, 1138, 1101, 1075, 1030, 995 $cm^{-1}$.

**4-Methyl-1-phenylimidazole (8).** A mixture of 4-methylimidazole (8.2 g, 0.10 mol), bromobenzene (23.5 g, 0.15 mol), anhydrous $K_2CO_3$ (14.0 g, 0.10 mol), and freshly prepared CuBr (0.60 g) in nitrobenzene (80 mL) was refluxed for 18 h according to the procedure of Pozharski.[34] The resulting solution was filtered and the filtrate acidified with concentrated HCl and nitrobenzene removed by steam distillation. The remaining aqueous solution was concentrated to 70 mL, neutralized with aqueous ammonia, and continuously extracted with ethyl acetate. The extract was dried ($Na_2SO_4$) and concentrated, and the residual oil was crystallized from petroleum ether to give 4-methyl-1-phenylimidazole as white crystals: mp 59.5–60.5 °C; 1.4 g (8.8 mmol, 8.8% yield); $^1H$ NMR ($CDCl_3$) $\delta$ 2.30 (s, 3H), 7.02 (s, 1H), 7.3–7.5 (m, 5H), 7.76 (s, 1H); $^{13}C$ NMR ($CDCl_3$) $\delta$ 13.6, 114.0, 120.9, 126.9, 129.6, 134.4, 137.4, 139.3; IR (KBr) 3153, 3095, 2916, 2856, 1596, 1505, 1474, 1462, 1445, 1387, 1363, 1286, 1263, 1255, 1210, 1161, 1066, 1003, 967, 912, 766, 741 $cm^{-1}$. Anal. Calcd for $C_{10}H_{10}N_2$: C, 75.92; H, 6.37; N, 17.71. Found: C, 75.76; H, 6.21; N, 17.80.

**3-(*N*-Phenylamino)propenenitrile (13).**[35] 3-Ethoxyacrylonitrile (19 g, 0.20 mol), aqueous ammonia (25 mL, 0.80 mol of ammonia), and aniline (14 g, 0.15 mol) were heated in an autoclave at 100 °C for 4 h. The resulting mixture was extracted with ether (3 × 25 mL) and the combined ether extracts were dried ($Na_2SO_4$), concentrated, and recrystallized (benzene) to give 3-(*N*-phenylamino)propenenitrile as a white solid: 5.0 g (0.045 mol, 30% yield). The product was further purified by sublimation (90 °C, 0.10 Torr) to give a white solid: mp 89.5–90.5 °C; $^1H$ NMR (DMSO-$d_6$) $\delta$ 4.23 (d, $J_{cis}$ = 8.7 Hz, 1H), 4.67 (d, $J_{trans}$ = 13.4 Hz, 1H), 6.9–7.3 (m, 10H), 7.48 (dd, $J$ = 8.7, 12.9 Hz, 1H), 7.87 (dd, $J$ = 13.4, 13.1, 1H), 9.51 (d, $J$=13.1 Hz, 1H), 9.74 (d, $J$ = 12.9 Hz, 1H); $^{13}C$ NMR (DMSO-$d_6$) $\delta$ 84.3, 86.9, 114.9, 115.5, 116.6, 121.2, 121.6, 121.9, 129.2, 129.4, 140.8, 141.3, 145.6, 146.9; IR (KBr) 3260, 3023, 2950, 2200, 1666, 1655, 1499, 1331, 1311, 1287, 1063, 953, 750 $cm^{-1}$.

**2-Methyl-3-(*N*-Phenylamino)propenenitrile (10).** 3-Amino-2-methylamino-propenenitrile[36] (0.41 g, 5.0 mmol) and aniline hydrochloride (1.3 g, 10 mmol) in methanol (25 mL) were refluxed for 5 h, cooled to room temperature, and diluted with water (25 mL). The resulting solution was extracted with ether (3 × 20 mL), the combined ether extracts were dried ($Na_2SO_4$) and concentrated, and the residue was treated with decolorizing carbon and recrystallized (benzene) to give 2-methyl-3-(*N*-phenylamino)propenenitrile: mp 142–143 °C, 0.48 g (3.3 mmol, 65% yield); $^1H$ NMR (DMSO-$d_6$) $\delta$ 1.81 (d, $J$ = 1.0 Hz, 3H), 6.8–7.5 (m, 5H), 7.54 (dd, $J$ = 12.8, 1.0 Hz, 1H), 8.73 (d, $J$ = 12.4, 1H); $^{13}C$ NMR (DMSO-$d_6$) $\delta$ 12.4, 76.6, 115.0, 121.3, 123.5, 129.2, 140.7, 141.5; IR (KBr) 2190, 2142, 1831, 1646, 1603, 1590, 1559, 1506, 1490, 760 $cm^{-1}$; UV ($CH_3CN$) $\lambda$ 303 nm (sh), $\lambda_{max}$ 282 ($\epsilon$ 29 600). Anal. Calcd. for $C_{10}H_{10}N_2$: C, 75.92; H, 6.37; N, 17.71. Found: C, 75.85; H, 6.20; N, 17.75.

**Irradiation and Analysis Procedures.** To monitor 1-phenylpyrazole to 1-phenylimidazole or *N*-(phenylamino)acrylonitrile photoconversion on an analytical scale, a solution of the appropriate 1-phenylpyrazole or *N*-(phenylamino)acrylonitrile (3.0 mL, 1.0 × $10^{-2}$ M or 10.0 mL, 1.0 × $10^{-2}$ M) in acetonitrile was placed in a quartz tube (7 mm i.d. or 14 mm i.d. × 13 cm long), that was sealed with a rubber septum and purged with nitrogen for 5 min prior to irradiation. The tubes were irradiated in a Rayonet photochemical reactor containing 3 (for **1**, **5**, and **6**) or 18 (for **4**) low-pressure Hg lamps. Preparative scale reactions were carried out by irradiating a nitrogen purged solution of the appropriate 1-phenylpyrazole (100 mL, 1.0 × $10^{-2}$ M) in acetonitrile in a quartz tube (23 mm i.d. × 30 cm long).

Formation of 1-phenylimidazoles was monitored by irradiating the appropriate 1-phenylpyrazole solution for 40 min while removing aliquots every 5 min (for **1**, **5**, and **6**) or for 7 h while removing aliquots every 1 h (for **4**) for GLC analysis on column A. Formation of acrylonitriles was monitored by irradiating the appropriate 1-phenylpyrazole solution for 15 min, concentrating the resulting solution (10 to 1), and analyzing the resulting solution by GLC on column B. Upon direct irradiation of a propenenitrile, reactant consumption was monitored by GLC on column B without concentration while 1-phenylimidazole formation was determined by GLC on column A. The retentions of all products are given relative to the appropriate starting reactant. Solutions resulting from preparative-scale reactions were concentrated to less than 0.5 mL. Unconverted reactants and products were collected by preparative GLC at the temperature indicated.

Quantitative GLC analysis of reactant consumption and product formation was accomplished by using calibration curves constructed for each reactant and product by plotting detector response versus a minimum of five standards of known concentrations. Correlation coefficients ranged from 0.993 to 0.999.

**1-Phenylpyrazole (1).** GLC analysis of the irradiated solution at 190 °C showed the formation of 1-phenylimidazole (**2**) with a relative retention of 2.2. GLC analysis of the concentrated solution at 170 °C showed the formation of 3-(*N*-phenylamino)propenenitrile (**3**) with a relative retention of 3.7.

**3-Methyl-1-phenylpyrazole (4).** GLC analysis of the irradiated solution at 190 °C showed the formation of 2-methyl-1-phenylimidazole (**7**) with a relative retention of 1.5.

**4-Methyl-1-phenylpyrazole (5).** GLC analysis of the irradiated solution at 190 °C showed the formation of 4-methyl-1-phenylimidazole (**8**) with a relative retention of 1.7. GLC analysis of the concentrated solution at 160 °C showed the formation of 2-methyl-3-(*N*-phenylamino)propenenitrile (**10**) with a relative retention of 6.3.

**5-Methyl-1-phenylpyrazole (6).** GLC analysis of the irradiated solution at 190 °C showed the formation of 5-methyl-1-phenylimidazole (**9**) with a relative retention of 2.0. GLC analysis of the concentrated solution at 185 °C showed the formation of 3-(*N*-phenylamino)-2-butenenitrile (**11**) with a relative retention of 5.8.

**3-(*N*-phenylamino)propenenitrile (3).** GLC analysis after 2 h of irradiation showed 4.9% consumption of **3** without formation of any volatile products.

**2-Methyl-3-(*N*-phenylamino)propenenitrile (10).** GLC analysis after 1 h of irradiation showed 5.0% consumption of **10** without formation of any volatile products.

**3-(*N*-phenylamino)-2-butenenitrile (11).** GLC analysis after 1.5 h of irradiation showed 5.3% consumption of **11** without formation of any volatile products.

**5-Methyl-4-deuterio-1-phenylpyrazole (6$d_1$).** A solution of **6$d_1$** (0.075 g in 25 mL of acetonitrile) in a quartz tube (20 mm i.d. × 15 cm long) was sealed with a rubber septum, purged with nitrogen for 5 min, and irradiated for 1 h in a Rayonet photochemical reactor equipped with 18 low-pressure Hg lamps. The acetonitrile was removed under reduced pressure. $^1H$ NMR (DMSO-$d_6$) of the resulting mixture of **6$d_1$** and **9$d_1$**

(33) Cornforth, J. W.; Cornforth, R. H. *J. Chem. Soc.* **1947**, 96–102.
(34) Pozharski, A. F.; Martsokha, B,K,; Simonov, A. M. *Zh. Obshch. Khim.* **1963**, *33*, 1005–1007; *Chem. Abstr.* **1963**, *59*, 7515e.
(35) Peeters, H.; Prange, V.; Vogt, W. Ger. Offen, 2,912,343; *Chem. Abstr.* **1981**, *94*, 102860p.
(36) Sieveking, H. U.; Luttke, W. *Angew. Chem., Int. Ed. Engl.* **1969**, *8*, 458–459.

showed a singlet at $\delta$ 7.74 (H-2 of $9d_1$) but no signal at $\delta$ 6.81 for a proton at C-4 of the 5-methyl-1-phenylimidazole.

**Determination of Quantum Yields.** Phototransposition quantum yields for **1**, **5**, and **6** were determined on acetonitrile solutions (20 mL, $1.00 \times 10^{-2}$ M) in quartz tubes (15 mm i.d. × 13 cm long) purged with nitrogen for 5 min prior to irradiation. Samples were irradiated in triplicate on a merry-go-round apparatus in a Rayonet reactor equipped with three low-pressure Hg lamps. In the case of **4**, the quantum yield was determined in triplicate by irradiating a nitrogen purged acetonitrile solution (100 mL, $1.00 \times 10^{-2}$ M) in a quartz tube (23 mm i.d. × 30 cm long) in the Rayonet reactor equipped with 18 low-pressure Hg lamps.

The phototransposition was monitored by GLC analysis (column A) to <10% conversion. Reactant consumption was determined from calibration curves of standard concentration versus peak area relative to biphenyl as an internal standard. Product formation was determined in the same manner with 3-nitro-1-phenylpyrazole as an internal standard.

Light intensities were determined by ferric oxalate actinometry ($\Phi_{254nm}$ = 1.28) according to published procedures.[14]

**Acknowledgment.** The authors gratefully acknowledge the Camille and Henry Dreyfus Foundation for support for the purchase of the DECstation and partial support for the purchase of the NMR spectrometer, the Perkin-Elmer Corp. for support in the form of equipment grants, and Dr. Arthur M. Halpern (Indiana State University) for measuring the fluorescence lifetimes.